

Time-Resolved EPR Characterization of a Folded Conformation of Photoinduced Charge-Separated State in Porphyrin–Fullerene Dyad Bridged by Diphenyldisilane

Yasuhiro Kobori,^{*,†} Yuki Shibano,^{*,§} Tsubasa Endo,[†] Hayato Tsuji,^{*,¶} Hisao Murai,[†] and Kohei Tamao^{*,‡}

Department of Chemistry, Faculty of Science, Shizuoka University, 836 Ohya Surugaku, Shizuoka 422-8529, Japan, and Institute for Chemical Research, Kyoto University, Uji, Kyoto 611-0011, Japan

Received September 17, 2008; E-mail: sykobor@ipc.shizuoka.ac.jp

For development of the molecular solar-energy conversion systems, it is crucial to investigate how both the molecular geometry and electronic structure of electron donor–bridge–acceptor (D–B–A) molecules contribute to the electronic coupling for the charge-separation (CS) and charge-recombination (CR) processes.^{1–4} Oligo- and polysilanes have been shown to possess such unique electronic properties that the σ -electrons are delocalized along the silicon framework (σ -conjugation).^{5,6} In very recent studies, molecular-wire^{7,8} character has been reported in the photoinduced electron-transfer (ET) processes of a series of zinc porphyrin–fullerenes bridged by oligosilane chains ZnP–[Si_n–C₆₀ (*n* = 1–5) at room temperature.⁹ Since the oligosilane chains are highly flexible, several molecular conformations exist.^{9–11} When the chain dynamics couple to the ET processes, roles of both the geometry and the electronic property on the electronic coupling may be hidden by the chain motions.⁹ Therefore, it is very important to characterize both the molecular geometry and the electronic property for each molecular conformation of D–B–A in frozen media.

In this study, we have characterized a specific folded geometry of the diphenyldisilane-linked porphyrin–fullerene dyad (ZnP–C₆₀, Figure 1) as well as its electronic properties by the time-resolved electron paramagnetic resonance (TREPR) measurements in a low temperature matrix. We show that the singly occupied molecular orbitals (SOMO) in the folded ZnP–C₆₀ are orthogonal to each other in the photoinduced CS state from the geometry and the exchange coupling of the radical pair (RP). This orbital conformation leads to prevention of the energy-wasting CR, although ZnP and C₆₀ are in close proximity.

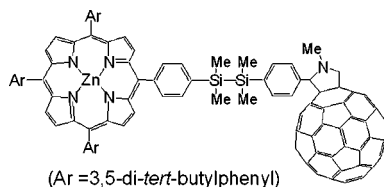


Figure 1. Structural formula of ZnP–C₆₀ bridged by diphenyldisilane.

Figure 2a shows the TREPR spectra obtained at different delay times after 532-nm laser irradiation of ZnP–C₆₀ (2×10^{-4} M) in a frozen (*T* = 91 K) benzonitrile. At the initial stage (0.2 μ s), a broad fine structure with an A/A/E/E polarization shape is detected (A and E denote microwave absorption and emission, respectively). This spectrum is

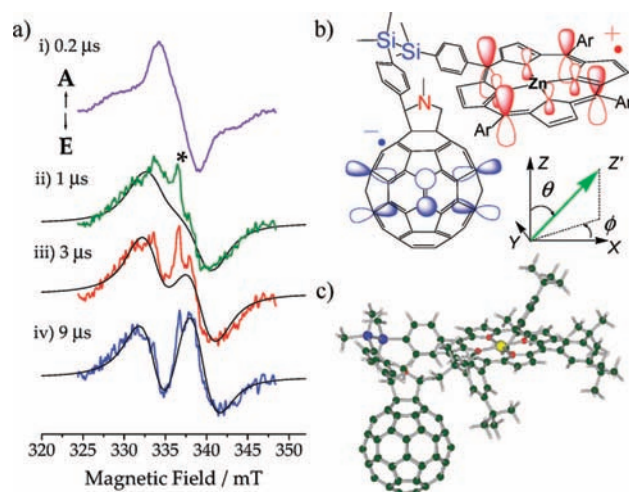


Figure 2. (a) TREPR spectra of ZnP–C₆₀ at different delay times after 532 nm laser irradiations at 91 K in benzonitrile. Black lines are simulated spectra of the RP in which the triplet–triplet polarization-transfer and spin relaxation effects are considered. (b) View of the molecular geometry and SOMOs of one of the folded conformations of ZnP–C₆₀ determined by the correlated RP simulations. The principal axes (*X*, *Y*, and *Z*) of the spin dipolar–dipolar interaction on the ³C₆₀ moiety and the dipolar–dipolar axis (*Z'*: green arrow) of the CS state are shown. (c) Molecular structure of (b) which was obtained by molecular mechanics calculation, showing consistency of position and orientation of the ZnP with respect to the C₆₀.

explained by the excited triplet state of fulleropyrrolidine,¹² showing that the triplet state of ZnP–³C₆₀* is initially created via the intersystem crossing of the excited singlet state, ZnP–¹C₆₀*.¹³ At 1 μ s in Figure 2a, the triplet signal mostly disappears while another broad A/E polarized component appears. In a dyad molecule composed of ZnP and C₆₀, an efficient intramolecular CS from ZnP to ³C₆₀* has been reported.¹³ The broad A/E feature is assigned to the fine structure that is due to an electron–electron dipolar splitting of the charge-separated state of ZnP^{•+}–C₆₀^{•–} (Supporting Information, SI) generated by the intramolecular CS of ZnP–³C₆₀*. From the entire line width of this spectrum, $|D| \approx 5$ mT is estimated as the dipolar splitting constant. From the point–dipole approximation, the distance between the two spins is calculated to be $r_{SS} \approx 0.8$ nm. This distance indicates that the origin of the A/E-type spectrum is the RP of one of the folded conformations, while the center-to-center distance (*r*) between ZnP and C₆₀ moieties is estimated to be 2.1 nm for the extended conformation.¹⁴ At the center positions of the TREPR spectra (* in Figure 2a), narrow A/E-polarized signals are superimposed on the broad A/E spectra. These narrow signals can be assigned to the CS state of the extended conformation.¹⁵ The broad A/E-type polarization in the CS state can be explained by the electron spin polarization transfer (ESPT)¹⁶ from ZnP–³C₆₀* to ZnP^{•+}–C₆₀^{•–}. At longer delay

[†] Shizuoka University.

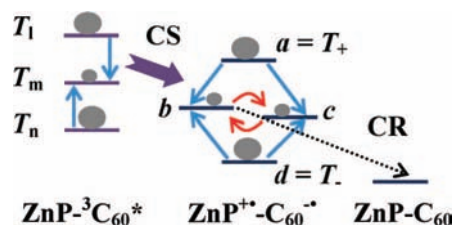
[‡] Kyoto University.

[§] Present address: Center for Future Laboratory, Kyushu University, 744 Motoooka, Nishi-ku, Fukuoka 819-0395, Japan.

[¶] Present address: Department of Chemistry, School of Science, The University of Tokyo, Bunkyo-ku, Tokyo 113-0033, Japan.

[‡] Present address: RIKEN Advanced Science Institute, 2-1 Hirosawa, Wako, Saitama 351-0198, Japan.

Scheme 1. Schematic Representations of EPR Transitions (Blue Arrows), Polarization Transfer via CS, the Spin Relaxations, and CR



times of 3 and 9 μs in Figure 2a, the spectrum pattern gradually changes to A/E/A/E, which is explained by a combination of sublevel-selective spin relaxation and CR³ in the spin correlated RP.¹⁷ (Scheme 1)

To clarify the molecular geometry of the CS state, we have modeled (1) the ESPT from the spin eigenstates of $\text{ZnP-}^3\text{C}_{60}^*$ to the eigenstates in the RP under the applied magnetic field¹⁶ and (2) kinetics of the spin–lattice relaxations and the singlet CR in the RP levels by using the density matrix method (see SI for details). To calculate the eigenfunctions (T_1 , T_m , and T_n in Scheme 1) and their populations under the applied magnetic field in $\text{ZnP-}^3\text{C}_{60}^*$, the dipolar splitting parameters of $D_T = -9.17$ mT and $E_T = -1.32$ mT were used from reported values for fulleropyrrolidine.¹⁸ Sublevel-selecting ratios for the S_1 – T_1 intersystem crossing were also considered to be $p_x = 0.67$, $p_y = 0.33$, and $p_z = 0.00$ for the T_x , T_y , and T_z levels, respectively.¹⁸ For the RP, the principal axis Z' of the spin dipolar interaction was represented by the polar angles (θ, ϕ) with respect to the principal axes (X , Y , and Z) of the dipolar interaction in $\text{ZnP-}^3\text{C}_{60}^*$ as shown in Figure 2b.¹⁸ $D = -5.2$ mT was used for the RP with $E = 0$. We considered that the CS state undergoes the S – T_0 mixing to create the spin-correlated RP¹⁷ (a , b , c , and d in Scheme 1). As a result of the spin polarization calculation, the A/E-type spectrum at 1 μs was reproduced, as shown by the solid line in Figure 2a, when $(\theta, \phi) = (34^\circ, 5^\circ)$ was utilized. According to the ESPT model,¹⁶ the spin polarization pattern depends on (1) the direction of the Z' axis in the X – Y – Z coordinate system and (2) the differences in p_x , p_y , and p_z . Thus, by using the triplet–triplet ESPT phenomenon via the photoinduced CS process, conformation of the CS state can be characterized with respect to the dipolar principal axes of the triplet state. Figure 2c shows one of the folded structures of ZnP-C_{60} geometrically optimized by the molecular mechanics calculation. The position of ZnP with respect to the C_{60} moiety is consistent with the polar angles of $(\theta, \phi) = (34^\circ, 5^\circ)$ described above. These results strongly support the validity of the geometry of the folded conformation (EPR conformation) characterized in the present study.

The gradual changes toward the A/E/A/E shape (3 and 9 μs in Figure 2a) were reproduced as shown by the solid lines by using $T_{bc} = 3.0$ μs and $k_{CR} = 2.0 \times 10^5$ s^{-1} , where T_{bc} and k_{CR} denote the relaxation time between the b – c populations (red arrows in Scheme 1) and the CR rate constant via the singlet RP, respectively. Together with the relaxation effects, spin–spin exchange coupling ($2J$) of +2.0 mT was required as the S – T energy gap to fully reproduce the three spectra (shown in Figure 2a) with a common set of parameters. The positive J is explained by the charge-transfer interaction as has been reported in numbers of CS systems.^{3,15,19} According to the model of the J , $2J$ has been approximated as $2J = |V|^2/\Delta E$, where $|V|$ and ΔE are the electronic coupling matrix element and the vertical energy gap for the CR, respectively.^{15,19,20} From $2J = 2.0$ mT, $|V| \approx 4$ cm^{-1} is estimated by $\Delta E \approx 1$ eV.³ In a CS state of a compact ZnP –fullerene dyad in which ZnP and C_{60} are in close proximity ($r = 0.76$ nm), $|V| \approx 200$ cm^{-1} has been specified as a through-space interaction.²¹ Since $|V| \approx 4$ cm^{-1} in

the present study is extremely small at $r_{SS} = 0.81$ nm which is estimated by $D = -5.2$ mT, it is concluded that the active SOMO is orthogonal to each other as shown by the π -orbitals^{4,22} in Figure 2b to suppress the electronic interaction. This orthogonal orbital relationship explains the small CR rate of $k_{CR} = 2.0 \times 10^5$ s^{-1} , indicating that the CR is inhibited due to the poor orbital overlap even at the short separation.^{23,24}

In conclusion, by means of the low-temperature TREPR, we have detected a specific folded conformation of the disilane-linked dyad ZnP-C_{60} with a small CR rate due to the orthogonal relationship of the SOMOs. This conformer should clearly be distinguished from the charge-transfer (CT) complex observed by the UV absorption measurements in the previous studies^{9,10} since such a CS state of the complex must have a large orbital overlap and is not detectable by the TREPR (SI). Among several molecular conformations, the structure in Figure 2c may play a crucial role as an entity to suppress the energy-wasting CR process.⁹ Further investigations are in progress to clarify the molecular geometries and $2J$ for the other $\text{ZnP-[Si}_n\text{]-C}_{60}$ systems.

Acknowledgment. This work was supported by a Grant-in-Aid for Scientific Research (No. 19614005) from Ministry of Education, Culture, Sports, Science and Technology, Japan. This research was partially carried out by using an instrument at the Center for Instrumental Analysis of Shizuoka University.

Supporting Information Available: Experimental details, optical spectroscopic data, and computation methods. This material is available free of charge via the Internet <http://pubs.acs.org>.

References

- Fukuzumi, S. *Phys. Chem. Chem. Phys.* **2008**, *10*, 2283–2297.
- Wasielewski, M. R. *J. Org. Chem.* **2006**, *71*, 5051–5066.
- Kobori, Y.; Yamauchi, S.; Akiyama, K.; Tero-Kubota, S.; Imahori, H.; Fukuzumi, S.; Norris, J. R. *Proc. Natl. Acad. Sci. U.S.A.* **2005**, *102*, 10017–10022.
- Yang, S. I.; Seth, J.; Balasubramanian, T.; Kim, D.; Lindsey, J. S.; Holten, D.; Bocian, D. F. *J. Am. Chem. Soc.* **1999**, *121*, 4008–4018.
- Tsuji, H.; Michl, J.; Tamao, K. *J. Organomet. Chem.* **2003**, *685*, 9–14.
- Tamao, K.; Tsuji, H.; Terada, M.; Asahara, M.; Yamaguchi, S.; Toshimitsu, A. *Angew. Chem., Int. Ed.* **2000**, *39*, 3287–3290.
- Choi, S. H.; Kim, B.; Frisbie, C. D. *Science* **2008**, *320*, 1482–1486.
- Davis, W. B.; Svec, W. A.; Ratner, M. A.; Wasielewski, M. R. *Nature* **1998**, *396*, 60–63.
- Sasaki, M.; Shibano, Y.; Tsuji, H.; Araki, Y.; Tamao, K.; Ito, O. *J. Phys. Chem. A* **2007**, *111*, 2973–2979.
- Tsuji, H.; Sasaki, M.; Shibano, Y.; Toganoh, M.; Kataoka, T.; Araki, Y.; Tamao, K.; Ito, O. *Bull. Chem. Soc. Jpn.* **2006**, *79*, 1338–1346.
- Michl, J.; West, R. *Acc. Chem. Res.* **2000**, *33*, 821–823.
- Da Ros, T.; Prato, M.; Guldi, D. M.; Ruzzi, M.; Pasimeni, L. *Chem.–Eur. J.* **2001**, *7*, 816–827.
- Luo, C.; Guldi, D. M.; Imahori, H.; Tamaki, K.; Sakata, K. *J. Am. Chem. Soc.* **2000**, *122*, 6535–6551.
- Shibano, Y.; Sasaki, M.; Tsuji, H.; Araki, Y.; Ito, O.; Tamao, K. *J. Organomet. Chem.* **2007**, *692*, 356–367.
- Di Valentin, M.; Bisol, A.; Agostini, G.; Fuhs, M.; Liddell, P. A.; Moore, A. L.; Moore, T. A.; Gust, D.; Carbonera, D. *J. Am. Chem. Soc.* **2004**, *126*, 17074–17086.
- Akiyama, K.; Tero-Kubota, S.; Ikoma, T.; Ikegami, Y. *J. Am. Chem. Soc.* **1994**, *116*, 5324–5327.
- Closs, G. L.; Forbes, M. D. E.; Norris, J. R. *J. Phys. Chem.* **1987**, *91*, 3592–3599.
- Bortolus, M.; Prato, M.; van Tol, J.; Maniero, A. L. *Chem. Phys. Lett.* **2004**, *398*, 228–234.
- Kobori, Y.; Sekiguchi, S.; Akiyama, K.; Tero-Kubota, S. *J. Phys. Chem. A* **1999**, *103*, 5416–5424.
- Anderson, P. W. *Phys. Rev.* **1959**, *115*, 2–13.
- Imahori, H.; Tkachenko, N. V.; Vehmanen, V.; Tamaki, K.; Lemmettyinen, H.; Sakata, Y.; Fukuzumi, S. *J. Phys. Chem. A* **2001**, *105*, 1750–1756.
- Zoleo, A.; Maniero, A. L.; Prato, M.; Severin, M. G.; Brunel, L. C.; Kordatos, K.; Brustolon, M. *J. Phys. Chem. A* **2000**, *104*, 9853–9863.
- Fukuzumi, S.; Kotani, H.; Ohkubo, K.; Ogo, S.; Tkachenko, N. V.; Lemmettyinen, H. *J. Am. Chem. Soc.* **2004**, *126*, 1600–1601.
- Small CS rate (ca. 10^6 s^{-1}) obtained by the rise in the SCRPR signal is explained by the small orbital overlap between one of the SOMOs of $^3\text{C}_{60}^*$ and the HOMO of ZnP , supporting the orthogonal orbital conformations in Figure 2b.

JA8073775